Molecular Crystals and Liquid Crystals
Publication details, including instructions for authors and subscription information:
http://www.tandfonline.com/loi/gmcl20

Effect of the Relative Orientation of the Two Fluoro-Substituents on the Mesophase Behavior of Phenylazophenyl Benzoates

M. M. Naoum [a], A. A. Fahmi [a] & H. A. Ahmed [a]
[a] Department of Chemistry, Faculty of Science, Cairo University, Cairo, Egypt
Version of record first published: 30 Jul 2012.

To cite this article: M. M. Naoum , A. A. Fahmi & H. A. Ahmed (2012): Effect of the Relative Orientation of the Two Fluoro-Substituents on the Mesophase Behavior of Phenylazophenyl Benzoates, Molecular Crystals and Liquid Crystals, 562:1, 43-65

To link to this article: http://dx.doi.org/10.1080/10426507.2012.660867

Mol. Cryst. Liq. Cryst., Vol. 562: pp. 43–65, 2012

ISSN: 1542-1406 print/1563-5287 online
DOI: 10.1080/10426507.2012.660867

Taylor & Francis
Taylor & Francis Group

Effect of the Relative Orientation of the Two Fluoro-Substituents on the Mesophase Behavior of Phenylazophenyl Benzoates

M. M. NAOUM,* A. A. FAHMI, AND H. A. AHMED

Department of Chemistry, Faculty of Science, Cairo University, Cairo, Egypt

Four novel types of laterally di-fluoro substituted 4-(2′-(or 3′-) fluoro phenylazo)-2-(or 3-) fluoro phenyl-4″-alkoxybenzoates were prepared and investigated for their mesophase behavior. In order to deduce the most probable conformation for each of the positional isomers investigated, the dipole moments for each of the four novel types have been determined experimentally in benzene at 30°C and compared with those theoretically calculated using molecular modeling program. Probable conformations deduced were found to vary according to the relative orientations of the two fluorine atoms. The results were used to correlate the mesophase behavior, in pure and mixed derivatives, with the conformation deduced for each series. The study aims to investigate the effect of the spatial orientation of the two lateral fluoro-substituents on the mesomorphic properties in their pure and mixed states.

Keywords Binary mixtures; dipole moments; fluorine; liquid crystals

1. Introduction

It is already known that the mesomorphic properties of nematic mesogens are strongly influenced when a lateral group is appended to a nematic core. The extent of such influence is dependent on the size, position, and polarity of the lateral substituent. Sterically, a lateral substituent widens the core and increases the intermolecular separation, which leads to a reduction in the lateral interactions [1–3] and hence the nematic stability is reduced. Gray [4] explained that an increase in the breadth of the molecules reduces both the nematic and smectic mesophase stability. It has been found [5] that the position of the fluoro-substituents in a given core unit can have marked effects on mesophase formation and transition temperatures, and melting and clearing points. Generally, fluorine substitution does not significantly change the overall shape of the core as a fluoro-substituent is only slightly larger than the hydrogen it replaces. So, such a study involves little change of the molecular shape, but changes do exist in the polarity and location of dipole moments. For example, mesophase type and transition temperatures were investigated [6–9] as a function of fluoro-substitution in 4-hexyloxy-4′-pentyl terphenyls, where the terminal chains and the core were the same in each material. Without any lateral fluoro-substituents, the low-polarity parent compound was found to exhibit smectic A and B phases. Incorporation of one fluoro-substituent in the central ring results in the introduction of a smectic C phase

*Address correspondence to M. M. Naoum, Department of Chemistry, Faculty of Science, Cairo University, Cairo, Egypt. E-mail: magdinaoum@yahoo.co.uk

and a nematic phase, and a massive reduction in the melting point. For the mono-fluoro terphenyl isomers, it has been shown that the phase sequence varies greatly with the location on the site of substitution. As the fluoro-substituents increase in number, there is a great tendency for the compound to exhibit the nematic phase. Melting points are often found to fall with increasing the degree and location of the fluoro-substitution.

The goal of the present investigation is to measure the dipole moments of the newly prepared laterally di-fluoro substituted isomers (**I***n*–**IV***n*) aiming, firstly, to deduce the most probable conformation for each of the differently, laterally substituted analogues. Secondly, it is to relate the mesophase behavior of the compounds, in pure and mixed states, with the apparent dipole moment (μ_{obs}), and consequently the deduced conformations, their calculated longitudinal (μ_Y) and lateral (μ_X) dipole moments, as well as the dipolar anisotropy of the molecule ($\Delta\mu = \mu_Y - \mu_X$).

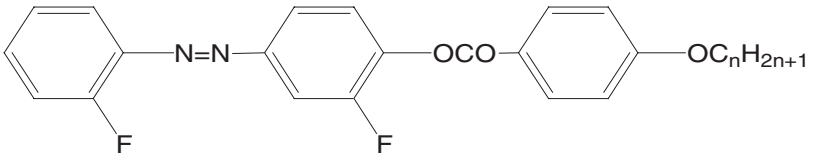

(I)

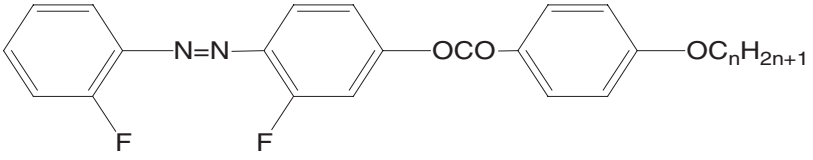

(II)

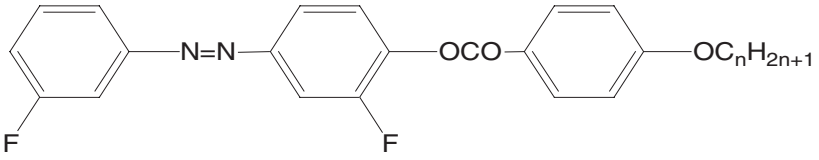

(III)

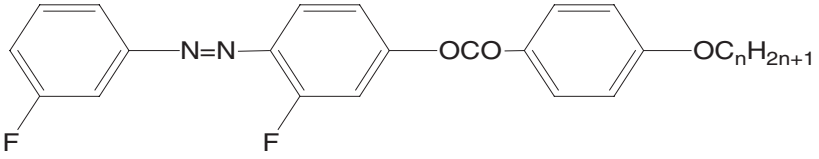

(IV)

2. Experimental

Chemicals were of very pure grades and purchased from the following companies: Buchs (Switzerland), Aldrich (Wisconsin, USA), E. Merck (Darmstadt, Germany), Alfa Aesar (Karlsruhe, Germany), and Acros (New Jersey, USA).

2.1. Preparation of Materials

Compounds **I***n*-**IV***n* were prepared according to the following scheme:

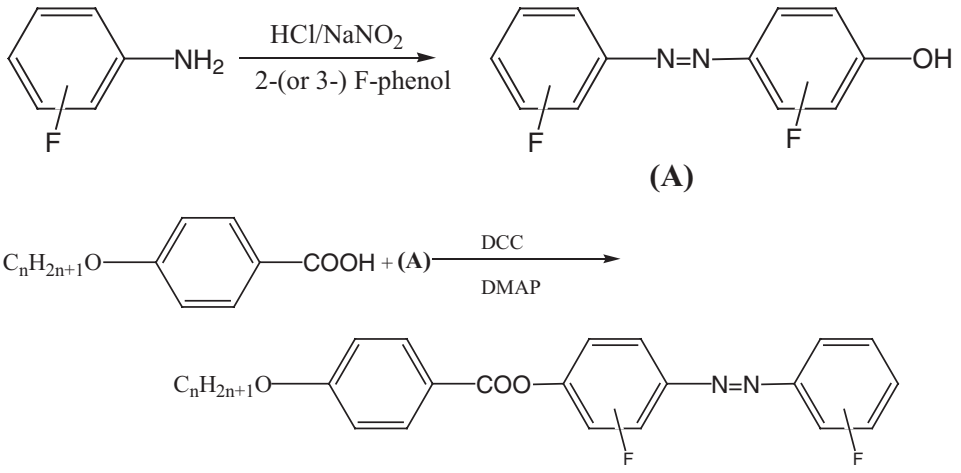

(I*n* - IV*n*)

2.1.1. Preparation of 4-(2′-(or 3′-) fluoro phenylazo)-2-(or 3-) fluoro phenol ***(A).*** The 2-(or 3-) fluoro aniline (0.05 mole) was dissolved in dilute hydrochloric acid and cooled in ice-salt bath to 0°C. To the resulting solution, a cold aqueous solution (0.05 mole) of sodium nitrite was added drop-wise with stirring. The cold mixture was then added slowly to a cold 2-(or 3-) fluoro phenol (0.05 mole) in sodium hydroxide solution (1:1). The mixture was further stirred at room temperature for 1 h, acidified with dilute hydrochloric acid, and the solid product obtained was filtered and recrystallized twice from glacial acetic acid to give pure compounds, as indicated by TLC analysis. The melting points, determined by DSC as sharp peaks, of the four prepared azo dyes **A** (substituted in positions 2′,2; 2′,3; 3′,2; and 3′,3) are 109.0°C, 112.9°C, 129.3°C, and 117.1°C, respectively.

2.1.2. Preparation of 4-(2′-(or 3′-) fluoro phenylazo)-2-(or 3-) fluoro phenyl-4″-alkoxybenzoates, ***I***n - ***IV***n. Molar equivalents of the 4-(2′(or 3′-) fluoro phenylazo)-2-(or 3-) fluoro phenol **(A)** and 4-*n*-alkoxybenzoic acid (0.05 mole each) were dissolved in 25 mL dry methylene chloride. To the resulting solution, two-molar equivalents of dicyclohexylcarbodiimide (DCC, 0.1 mole) and few crystals of 4-(dimethylamino)pyridine (DMAP), as catalyst, were added and the solution was stirred for 72 h at room temperature. The solid was filtered off and the solution was evaporated. The solid product was recrystallized twice from acetic acid and twice from ethanol to give pure products, as indicated by TLC analysis, and sharp melting and clearing peaks in their DSC thermograms.

2.2. Physical Characterization

Calorimetric measurements were carried out using a PL-DSC (Polymer Laboratories, England). The instrument was calibrated for temperature, heat, and heat flow according to the method recommended by Cammenga et al. [10]. The measurements were carried out for

small samples (2–3 mg) placed in sealed aluminum pans. All of the thermograms have been achieved at a heating rate of 10°C/min in an inert atmosphere of nitrogen gas (10 mL/min).

Transition temperatures were checked and types of mesophases identified for compounds prepared by standard polarized-light microscopy (PLM) of Wild, Germany, attached to a home-made hot-stage. The temperature was measured by a thermocouple attached to a temperature controller (Brookfield, England).

Thin layer chromatography was performed with TLC sheets coated with silica gel (E. Merck); spots were detected by UV irradiation.

Infrared spectra (4000–400 cm^{-1}) were measured with a Perkin Elmer B25 spectrophotometer, and ^1H NMR-spectra with a Varian EM 350L.

For dipole moment determination, static dielectric constants, ε', were measured with a WTW Dipolemeter type DM 01, Germany. Refractive indices were measured by an Abbe Refractometer (made by Bellingham and Stanley Limited, England).

For the construction of binary phase diagrams, the mixtures of the two components were prepared to cover the whole range of composition. Transition temperatures obtained for all prepared blends, as measured by both DSC and PLM, agreed within 2°C–3°C. In the phase diagrams, constructed by plotting transition temperatures *versus* mixture composition, the symbol "o" denotes solid-mesophase, "□" mesophase-isotropic transitions, "•" mesophase-another mesophase, and, "▲" the eutectic temperature.

2.3. Measurement of Dipole Moments

Analytical grade benzene was purified according to the recommended procedure [11]. Since the dipole moments of all members of a homologous series are the same independent of the length of the terminal alkoxy-chain (*n*), the dipole moments of the isomers **I***12*-**IV***12* were experimentally determined as examples.

Five dilute solutions of the compound in benzene were prepared with weight fractions ranging from 10^{-3} to 10^{-2}. The dielectric constants, densities, and refractive index were measured for each solution at 30°C, and the dipole moments were calculated as described earlier [12]. On the basis of the precisions in the measurements of dielectric constants (±0.0005), densities (±0.0001), refractive indices (±0.001), and solution concentrations (±0.02%), the dipole moment values obtained are believed reliable to ±0.05 D.

3. Results and Discussion

3.1. Confirmation of Molecular Structure

Infrared spectra, mass spectra, and elemental analyses for compounds investigated were consistent with the structures assigned. ^1H NMR data showed the expected integrated aliphatic to aromatic proton ratios in all compounds investigated. Representative infrared, mass, and ^1H NMR spectra are given in Tables 1–3, respectively.

3.2. Mesophase Behavior of Simple Molecules

The phase transition temperatures and enthalpies of the prepared compounds (**I***n*–**IV***n*) are given in Table 4. These data are represented graphically in Fig. 1 as a function of the alkoxy-chain length. As can be seen from Fig. 1, for the four homologous series investigated there is no systematic pattern of melting behavior with the increase of the terminal alkoxy-chain length. With respect to their mesophase behavior, the type of phase or phases observed

Table 1. Infrared spectra of some representative examples

Comp. no.	ν_{CH3} Asym.	ν_{CH3} Sym.	$\nu_{C=O}$	$\nu_{C=N}$	ν_{C-O}	ν_{C-O}
I*16*	2920	2854	1744	1600	1483	1238
II*8*	2926	2859	1727	1602	1481	1257
III*12*	2921	2852	1732	1600	1487	1258
IV*10*	2922	2854	1731	1602	1480	1243

depends mainly upon the location and orientation of the two fluoro-substituents. Thus, when the two fluorine atoms are located, in both rings, pointing toward the core of the molecule (i.e., both in position-2, as in homologues **I***n*; Fig. 1(a)), the nematic phase is favored covering the whole series except the highest homologue **I***16*, which is purely smectogenic possessing the SmC as the only mesophase observed. Conversely, when the two fluoro-substituents are located in both rings away from the core (i.e., both in position-3, as in homologues **IV***n*; Fig. 1d), the smectic C phase predominates except for the lower two homologues **IV***8* and **IV***10*, which are dimorphic and exhibit a narrow nematic phase range. In the homologous series **II***n*, where the fluoro-substituent is located in the terminal ring pointing towards the core, while the other is located in the central ring away from the core (i.e., in positions 2 and 3, respectively, Fig. 1b), the lower two homologues (**II***8* and **II***10*) are purely nematogenic, while the higher three (**II***12*, **II***14*, and **II***16*) are purely smectogenic, possessing the SmC phase. Finally, in the homologous series **III***n*, where the location of the two fluoro-substituents are the reverse of series **II***n* (i.e., they are located in positions 3 and 2, respectively; Fig. 1c), the nematic phase predominates irrespective of the terminal alkoxy-chain length.

In order to confirm that the nematic phase is the only mesophase exhibited by all the homologues **III***n*, a binary phase diagram was constructed (Fig. 2(a)) between homologue **III***8*, as an example, and the purely nematogenic 4-hexyloxybenzoic acid, which exhibits the enantiotropic nematic phase. In a similar way, in order to confirm that the SmC phase predominates in the homologues **IV***n*, a binary phase diagram was constructed (Fig. 2(b)) between homologue **IV***16*, as an example, and the purely smectogenic 4-hexadecyloxybenzoic acid, which exhibits the enantiotropic SmC phase. Both diagrams indicated that the nematic and smectic C phases are the only mesophases observed in the compounds investigated. This will be further confirmed for the other homologues from the binary mesophase behavior of mixed isomers.

Table 2. Mass spectra (*m/z*) of the representative derivatives (**I***n*–**IV***n*)

Compound	*n*	Whole Structure	$C_nH_{2n+1}OC_6H_4CO-$	$-OC_6H_4CO-$
I*16*	16	578	345	121
II*8*	8	466	233	121
III*12*	12	522	289	121
IV*10*	10	494	261	121

Table 3. [1]H-NMR spectra of some representative examples

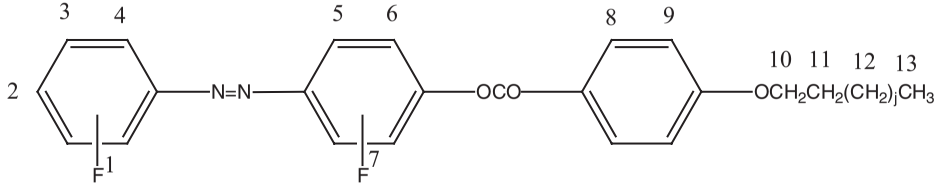

Compound	*n*	1 t,3H	2 m,2H	3 d,2H	4 d,2H	5 d,2H	6 d,2H	7 d,2H	8 d,2H	9 d,2H	10 t,2H	11 q,2H	12 m,2jH	13 t,3H
I*16*	16	7.15	7.45	7.21	7.88	7.76	7.34	7.70	8.05	6.91	3.93	1.73	1.27	0.95
II*8*	8	7.15	7.44	7.30	7.89	7.99	7.12	7.10	8.04	6.89	3.91	1.75	1.28	0.95
III*12*	12	7.66	7.15	7.45	7.69	7.77	7.34	7.73	8.01	6.91	3.95	1.75	1.28	0.94
IV*10*	10	7.62	7.20	7.41	7.71	8.01	7.11	7.09	8.01	6.91	3.95	1.75	1.28	0.94

Table 4. Phase transition temperatures (T,°C), enthalpy of transition (ΔH, kJ/mole), and entropy (ΔS, J/mol/K) for the homologous series **I***n*–**IV***n*

Comp. no.	*n*	$T_{Cr–C}$ ($\Delta H_{Cr–C}$)	$T_{Cr–N}$ ($\Delta H_{Cr–N}$)	$T_{C–N}$ ($\Delta H_{C–N}$)	$\Delta S_{C–N}$	$T_{C–I}$ ($\Delta H_{C–I}$)	$\Delta S_{C–I}$	$T_{N–I}$ ($\Delta H_{N–I}$)	$\Delta S_{N–I}$
I*8*	*8*	—	71.3 (40.8)	—	—	—	—	99.9 (0.78)	2.1
II*8*		—	87.3 (18.1)	—	—	—	—	95.9 (0.51)	1.4
III*8*		—	95.5 (67.2)	—	—	—	—	102.1 (1.44)	3.8
IV*8*		86.8 (103.1)	—	116.6 (10.9)	28.0	—	—	119.8 (2.3)	5.9
I*10*	*10*	—	86.0 (52.6)	—	—	—	—	99.3 (0.93)	2.5
II*10*		—	82.2 (35.6)	—	—	—	—	81.2 (0.87)*	2.5
III*10*		—	92.9 (94.5)	—	—	—	—	101.8 (1.42)	3.8
IV*10*		80.7 (45.5)	—	117.3 (5.3)	13.6	—	—	118.5 (1.91)	4.9
I*12*	*12*	—	92.0 (53.0)	—	—	—	—	99.1 (0.98)	2.6
II*12*		77.9 (27.0)	—	—	—	87.2 (1.31)	3.6	—	—
III*12*		—	82.9 (55.5)	—	—	—	—	101.5 (1.03)	2.7
IV*12*		72.5 (60.9)	—	—	—	117.3 (8.53)	21.8	—	—
I*14*	*14*	—	88.9 (31.4)	—	—	—	—	96.5 (1.04)	2.8
II*14*		100.8 (21.3)		—	—	89.1* (1.2)	3.3		—
III*14*		—	96.2 (24.2)	—	—	—	—	99.3 (0.64)	1.7
IV*14*		97.9 (27.8)	—	—	—	114.3 (1.91)	4.9	—	—
I*16*	*16*	87.0 (70.7)	—	—	—	90.4 (1.69)	4.6	—	—
II*16*		99.1 (62.9)	—	—	—	89.7 (0.65)*	1.8	—	—
III*16*		—	65.4 (172.9)	—	—	—	—	97.0 (15.32)	4.1
IV*16*		96.1 (73.1)	—	—	—	112.2 (3.72)	9.7	—	—

*Denotes monotropic phase.

Note. Cr, solid crystal; N, nematic; C, smectic c; and I, isotropic.

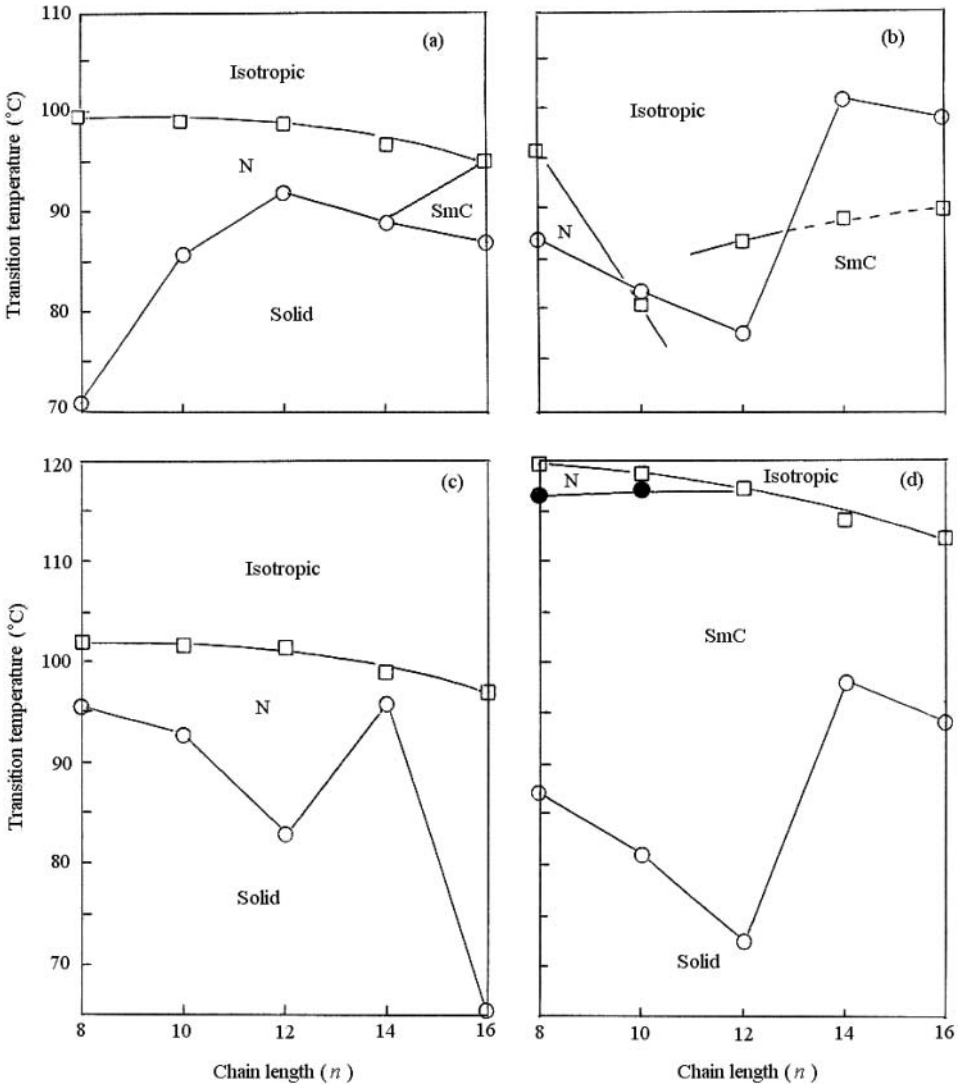

Figure 1. Effect of the alkoxy-chain length (*n*) on the mesophase behavior of the derivatives **I***n*-**IV***n*: (a) **I***n*, (b) **II***n*, (c) **III***n*, and (d) **IV***n*.

Since the mesophase stability of a liquid crystalline compound is mainly dependent upon the intermolecular attractions, in which molecular polarity plays a significant role, it has been shown [13] that in a series of compounds the dipole moment of any compound is dependent upon the nature and location of the substituent. A change in the extent of electronic interactions between the substituent and the remainder of the molecule alters the polarizability and resultant dipole moment of the molecule. It has also been shown [14,15] that the dipole moments of all members of a homologous series are virtually the same irrespective of the alkoxy-chain length. This result is in accordance with the fact that the alkoxy groups are of the same polarity regardless of length and, at the same time, do

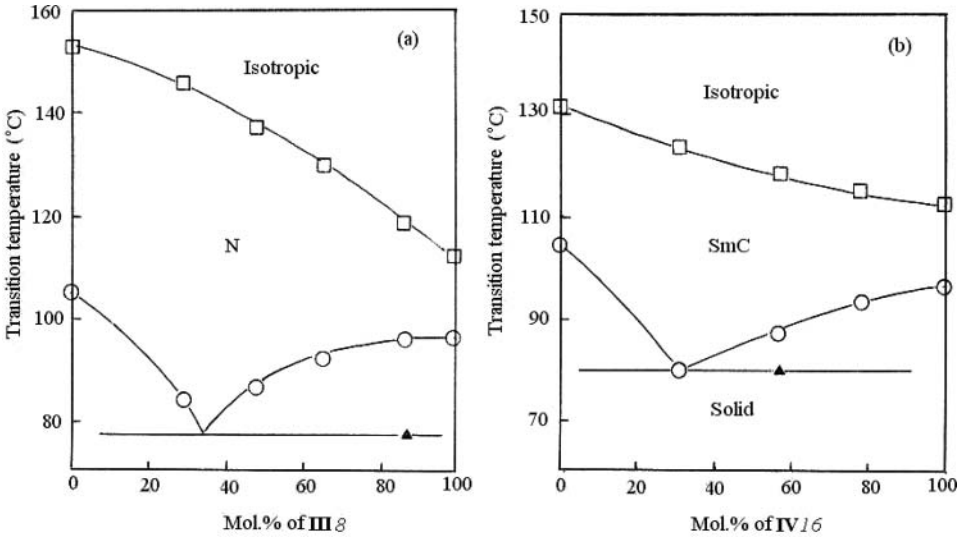

Figure 2. Confirmation of the mesophase of selected homologues: (a) **III***8*/hexyloxy benzoic acid, and (b) **IV***16*/hexadecyloxy benzoic acid.

not affect the extent of conjugative interactions between the alkoxy oxygen and the ester carbonyl, as is confirmed by infrared spectra.

Polarization and dipole moment data for compounds **I***n*–**IV***n* in benzene at 30°C are summarized in Table 5. The symbols have the following meanings: ${}_{D}P_2$ is the molar deformation polarization of the solute obtained by extrapolating the measured molar refraction for the sodium-D line to infinite wavelength [16], $P_{2\infty}$ is the molar polarization of the solute at infinite dilution taken as the average of that determined graphically and those of Hedestrand's [17] and Palit-Banerjee's [18] equations, and μ(D) is the dipole moment determined by the refractivity method form:

$$\mu(\mathrm{D}) = 0.01273\sqrt{[(P_{2\infty} - {}_{D}P_2)T]}$$

3.3. Deduction of the Most Probable Conformations

Generally, there is a possibility for rotation of any of the three benzene rings around their 1,4-axes. But, this may take place in cases where the concerned molecule comprises a biphenyl

Table 5. Polarization data for compounds **I***10*–**IV***10*

Comp.	${}_{D}P_2$ (Cm^3)	Graph.	Hedestrand				Palit-Ban.		Guggenheim			μ_{obs} (D)
			$P_{2\infty}$	α	β	μ	γ	μ	Δ	α	μ	
I*10*	181.9	3.5	472.0	3.6	0.2	3.7	1.94	2.40	3.2	3.6	3.80	3.35
II*10*	516.4	5.5	887.0	12.5	2.3	5.21	0.72	4.95	11.0	12.5	5.43	5.27
III*10*	363.9	2.8	485.0	5.6	1.1	3.35	0.47	3.40	5.2	5.6	3.32	3.21
IV*10*	353.3	5.9	953.0	9.9	0.7	5.51	0.64	5.75	9.2	9.9	5.50	5.63

or terphenyl moiety [5,19]. In the present case, however, the molecules are connected by ester and azo groups. In fact, the ester group contains no multiple bonds in the chain of atoms actually linking the benzene rings; however, conjugative interaction within the ester group and the rings does lead to some double bond character and stiffer structure than might be expected [20]. In our case, if the central ring is out of plane, the conjugative interaction between both linking groups and the rings will not be allowed and consequently the polarizability of the whole molecule will be too much disrupted and destroy any possible mesophase formation. All members of the four homologous series (**I***n*-**IV***n*) are mesomorphic, hence they should all exist in planar linear conformations. Accordingly, we are going to limit ourselves to the calculation of the theoretical dipole moments, using the molecular modeling program [21], only to all possible planar conformations; these are represented in Scheme 1 by the conformations ***1–8***. The results of computation for the

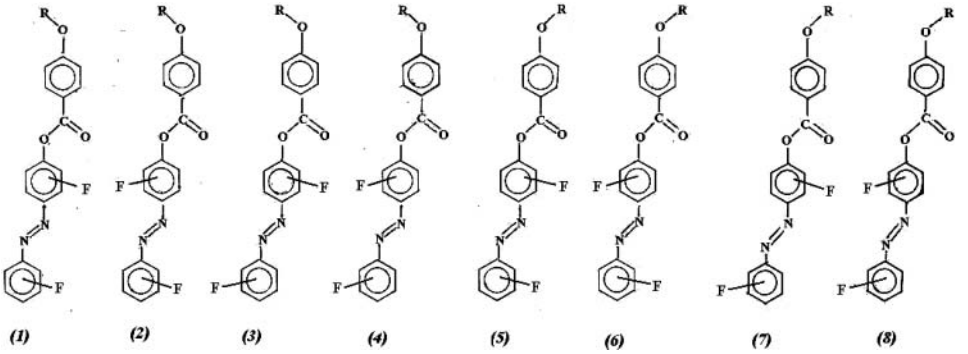

Scheme 1. Various possible planar conformations assigned for the homologous systems **I***n*–**IV***n*.

eight possible planar conformers, for the four homologous series **I***n*–**IV***n*, are collected in Table 6, together with the experimentally determined apparent dipole moment values, μ_{obs}. As given in Table 6, the most probable conformation for each homologous series varies according to the location and orientation of the fluoro-substituent. The dipole moment components, μ_X and μ_Y, for each homologous series are calculated by the same program and the most probable conformations deduced, and the values are collected in Table 7. The dipole moment component, μ_Y, is that calculated along the long axis of the molecule, and μ_X is accordingly the perpendicular, lateral component in such a way that $\mu_{obs}{}^2 = \mu_X{}^2 + \mu_Y{}^2$.

In order to investigate the effect of dipole moment on the stability of the mesophase exhibited by compounds **I***n*-**IV***n*, values of $\sqrt{T}_C$ are plotted as function of the observed

Table 6. Dipole moments (D) calculated for conformations (***1–8***) for compounds of series **I***n*--**IV***n*

Comp.	μ_{obs}	*1*	*2*	*3*	*4*	*5*	*6*	*7*	*8*
I*n*	3.35	5.28	2.62	2.62	0.94	2.95	1.39	1.39	3.20
II*n*	5.27	5.24	2.56	2.56	0.73	2.61	0.24	0.24	2.88
III*n*	3.21	5.25	2.56	2.55	0.74	2.62	0.24	0.24	2.89
IV*n*	5.63	5.67	3.34	3.33	2.27	3.15	1.78	1.78	3.38

Table 7. Calculated dipole moments (μ_{calc}) of the most probable conformations for the homologous series, **I***n*–**IV***n*, with their longitudinal (μ_Y) and lateral (μ_X) components, and anisotropy of dipole moment ($\Delta\mu$)

Series	Conform.	μ_{calc}	μ_Y	μ_X	$\Delta\mu$
I*n*	***8***	3.20	3.15	0.17	2.98
II*n*	***1***	5.24	5.23	0.60	4.7
III*n*	***8***	2.89	2.85	0.20	2.65
IV*n*	***1***	5.67	5.53	0.26	5.27

dipole moments, μ_{obs} in Fig. 3. As can be seen from Fig. 3, the $\sqrt{T_C}$ linearly, but slightly, decreases with the total dipole moment of the compound. Contrary to the effect of the terminal substituent, the weak negative $\sqrt{T_C}$ dependency on the dipole moment may be attributed first to the negligible steric interaction of the lateral fluoro-substituent, second,

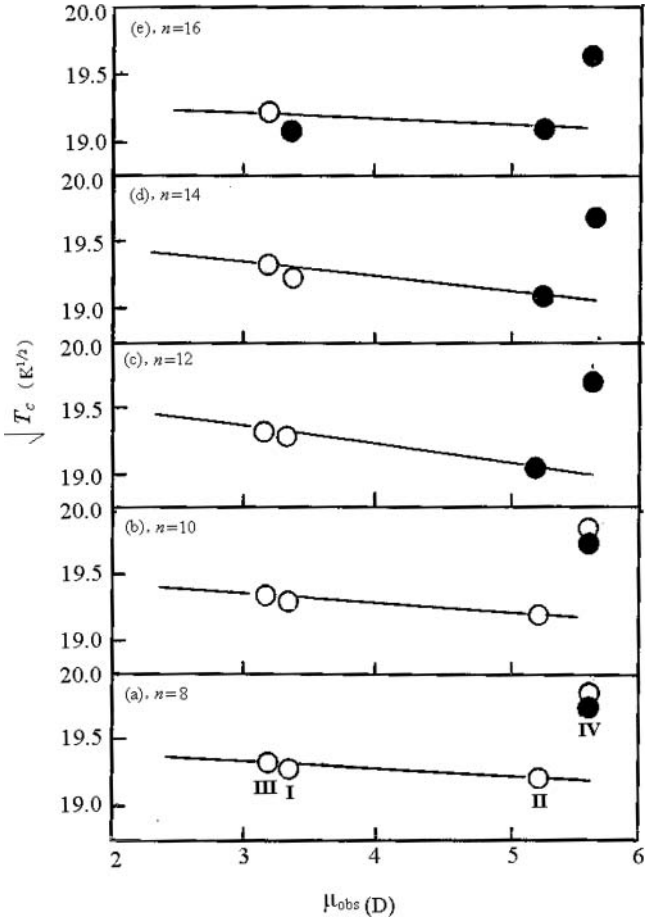

Figure 3. Dependence of $\sqrt{T_C}$ on the observed dipole moment of the homologous series **I***n*-**IV***n*: (a) $n = 8$, (b) $n = 10$, (c) $n = 12$, (d) $n = 14$, and (e) $n = 16$.

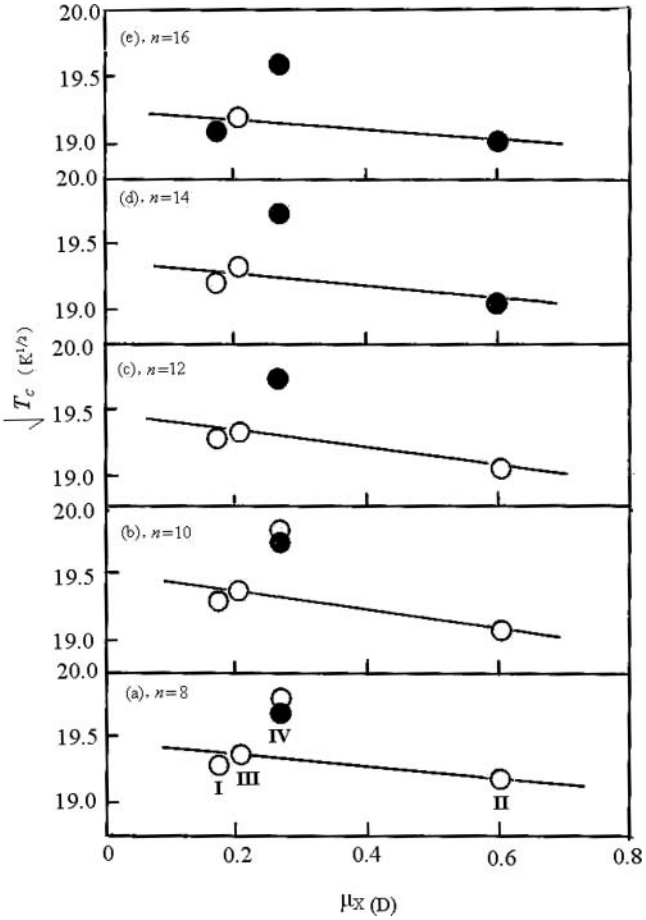

Figure 4. Dependence of $\sqrt{T}_C$ on the lateral dipole moment component, μ_X, calculated for the homologous series **I***n*–**IV***n*: (a) $n = 8$, (b) $n = 10$, (c) $n = 12$, (d) $n = 14$, and (e) $n = 16$.

to the weak conjugative interaction with the mesogenic portion of the molecule, and third, to the weak dipole–dipole repulsion as a consequence of the parallel alignment of the rod-shaped molecules. In order to decide which component of the dipole moment is more pronounced on the lateral interaction between neighboring molecules that leads to stabilization of the mesophase, values of $\sqrt{T}_C$ are once plotted as function of the lateral, μ_X, and another against the longitudinal, μ_Y, components of the dipole moments in Figs 4 and 5, respectively. Comparison between figures with Fig. 3 reveals that the dependency on either of the dipole moment components, μ_X or μ_Y, parallels that of the total dipole moment. Such a destabilization effect (the negative slope) varies irregularly and slightly with the increase of the terminal alkoxy-chain length. Since the anisotropy of molecular structure is generally reflected into a dipolar anisotropy ($\Delta\mu = \mu_Y - \mu_X$), it would be worthy to investigate the effect of the latter value on the mesophase behavior of the compounds (Fig. 6). Again, as can be seen from Fig. 6, the mesophase stability decreases with $\Delta\mu$. A common feature observed from Figs 3–6 is that the mesophase stability of the homologues **IV***n* is always much above the linear dependency. This may be attributed to a face-to-face

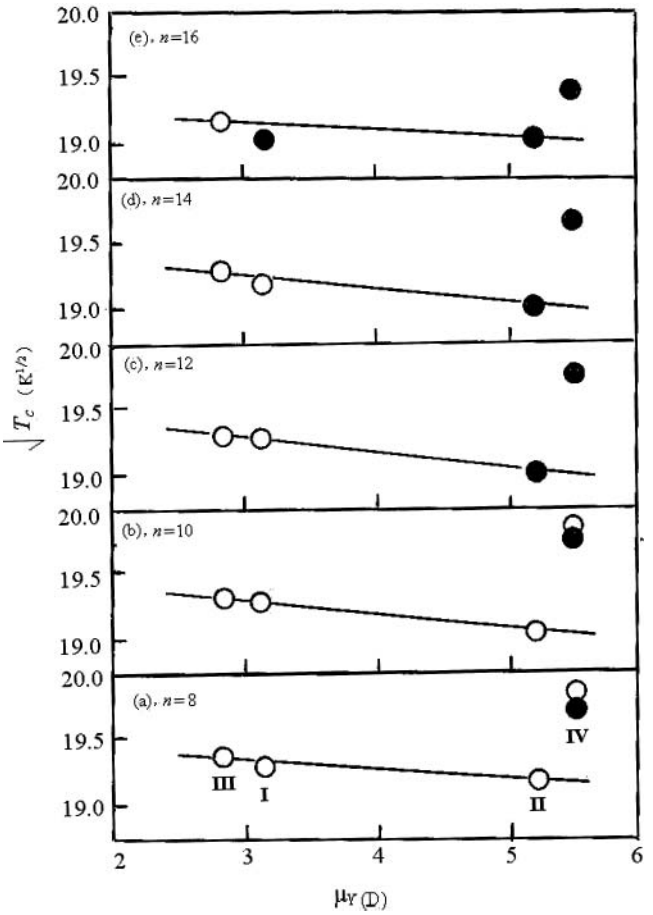

Figure 5. Dependence of $\sqrt{T}_C$ on the longitudinal dipole moment component, μ_Y, calculated for the homologous series **I***n*–**IV***n*: (a) $n = 8$, (b) $n = 10$, (c) $n = 12$, (d) $n = 14$, and (e) $n = 16$.

alignment of the rod-shaped molecules existing in conformation ***1*** that leads to increased lateral adhesion and consequently greater nematic stability, in the lower homologues ($n =$ 8 and 10), and the appearance of the SmC phase in all homologues of group **IV**.

3.4. Orientation of Lateral Fluorine and Entropy Change of Transition

The entropies of the nematic–isotropic (○), smectic–isotropic (●), or smectic C–nematic (□) transitions were calculated for all members of the four series **I**–**IV** and the results are shown in Table 4, and represented graphically as a function of the alkoxy-chain length in Fig. 7. Since the homologues **I***n* exist in the conformation ***8*** in which the two fluorine atoms are situated together on one side of the conformer but opposite to the ester C=O group, the lateral dipole moment component ($\Delta\mu_X = 0.17$ D) is small and the apparent dipole moment (3.2 D) is relatively small. Hence, the entropy change ($\Delta S_{N\text{-}I}$, Fig. 7(a)) increases slightly with n up to $n = 12$ carbons, and due to the increased lateral adhesion with increase of alkoxy-chain length to $n = 16$, the entropy change jumps to 4.9 J/mol/K as a result of the formation of the more ordered SmC phase. With respect to the homologues **II***n*, they exist in conformation ***1***

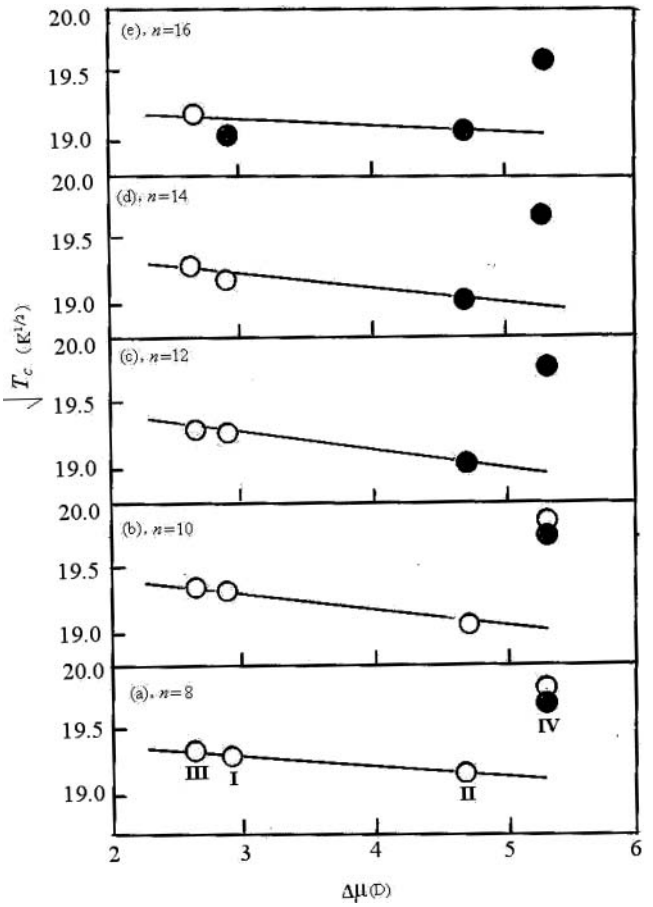

Figure 6. Dependence of $\sqrt{T_C}$ on the dipolar anisotropy, $\Delta\mu$, calculated for the homologous series **I***n*–**IV***n*: (a) $n = 8$, (b) $n = 10$, (c) $n = 12$, (d) $n = 14$, and (e) $n = 16$.

with the lateral fluorine atoms attached to one and the same side that carries the ester C=O group of the conformer. Such an arrangement has led to the increase of the lateral dipole moment component ($\Delta\mu_X$) to 0.6 D and an apparent dipole moment value of 5.24 D. These enhanced dipole moment values facilitate the generation of the SmC phase starting from the homologue **II***12*. Similar to homologues **I***n*, the homologues **III***n* exist in the conformer ***8*** with lower dipole moment values ($\Delta\mu_X = 0.2$ and $\mu_{obs} = 2.89$ D). The mesophase observed in all homologues investigated were of the SmC type and the entropy changes during phase transition are relatively small. Alternatively, the homologues **IV***n* resemble those of **II***n* in which they exhibit in the conformation ***I*** and have apparent dipole moment values of 5.67 D. Accordingly, the lower homologues, **IV***8* and **IV***10*, are dimorphic possessing both SmC and N mesophases with relatively high entropy of transitions. Higher homologues are purely smectogenic with high entropy change (e.g., $\Delta S_{C–I} = 28.0$ and 21.8 J/mol/K for the homologue **IV***8* and **IV***12*, respectively). Alternatively, when comparison is made between isomers of the four series, i.e., bearing similar alkoxy groups, $\Delta S_{N–I}$ decreases in an order that differs according to the relative orientation of the two lateral fluorine substituents. Thus,

for $n = 8$, ΔS_{N-I} decreases in the order:
IV > **III** > **I** > **II**;
for $n = 10$, ΔS_{N-I} decreases in the order:
III > **IV** > **II** > **I**;
for $n = 12$, ΔS_{N-I} decreases in the order:
IV > **III**, while ΔS_{C-I} for **I** > **II**; and
for $n = 16$, ΔS_{C-I} decreases in the order:
IV > **I** > **II**.

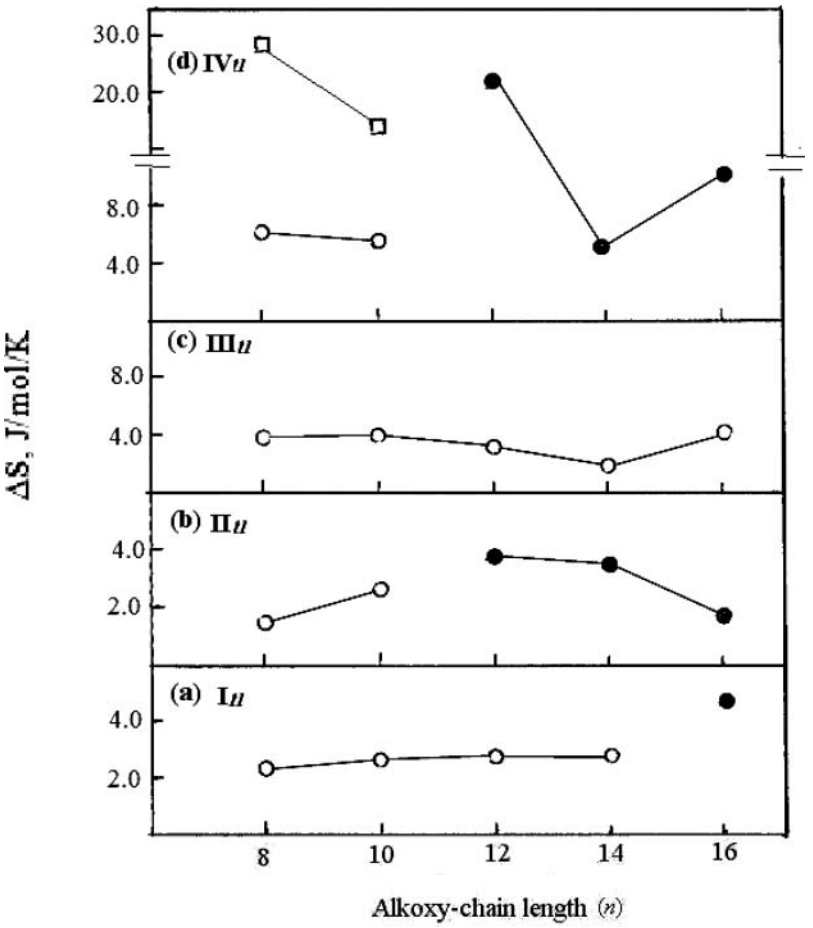

Figure 7. Entropy change of transition (ΔS) as a function of alkoxy-chain length (n).

3.5. Mesophase Behavior of Binary Mixtures

Turning now to the investigation of the mesophase behavior of mixed systems, we have to limit such investigation to binary mixtures of isomeric components bearing the same alkoxy-chain but differing in the position of the fluoro-substituents. This still leads to a great number of phase diagrams. So, it seems sufficient to investigate, as examples, mixtures with isomeric components bearing extreme alkoxy-chain length, namely, $n = 8$ and 16 carbons.

*3.5.1. Binary Mixtures of Isomers, **I**n /**II**n.* The binary phase diagrams of the two binary systems, each made from the two isomers from series **I***n* and **II***n*, are illustrated for $n =$ 8 and 16 in Fig. 8. As can be seen from the figure, in the binary mixture of the lower homologues **I***8*/**II***8*, since both components are nematogenic, their binary mixture forms an ideal solution in which linear T_{N-I} composition dependence is observed. In the higher homologous system (**I***16*/**II***16*), the SmC predominates since both components are smectogenic (SmC) and, consequently, ideal mesophase behavior takes place as evidenced by the linear T_{C-I} composition dependence. Such an ideal mesophase behavior may be attributed to a back-to-face arrangement of molecules existing between the conformation ***8*** (for the homologues **I***n*) and conformation ***1*** (for the homologues **II***n*; see Fig. 8). With respect to

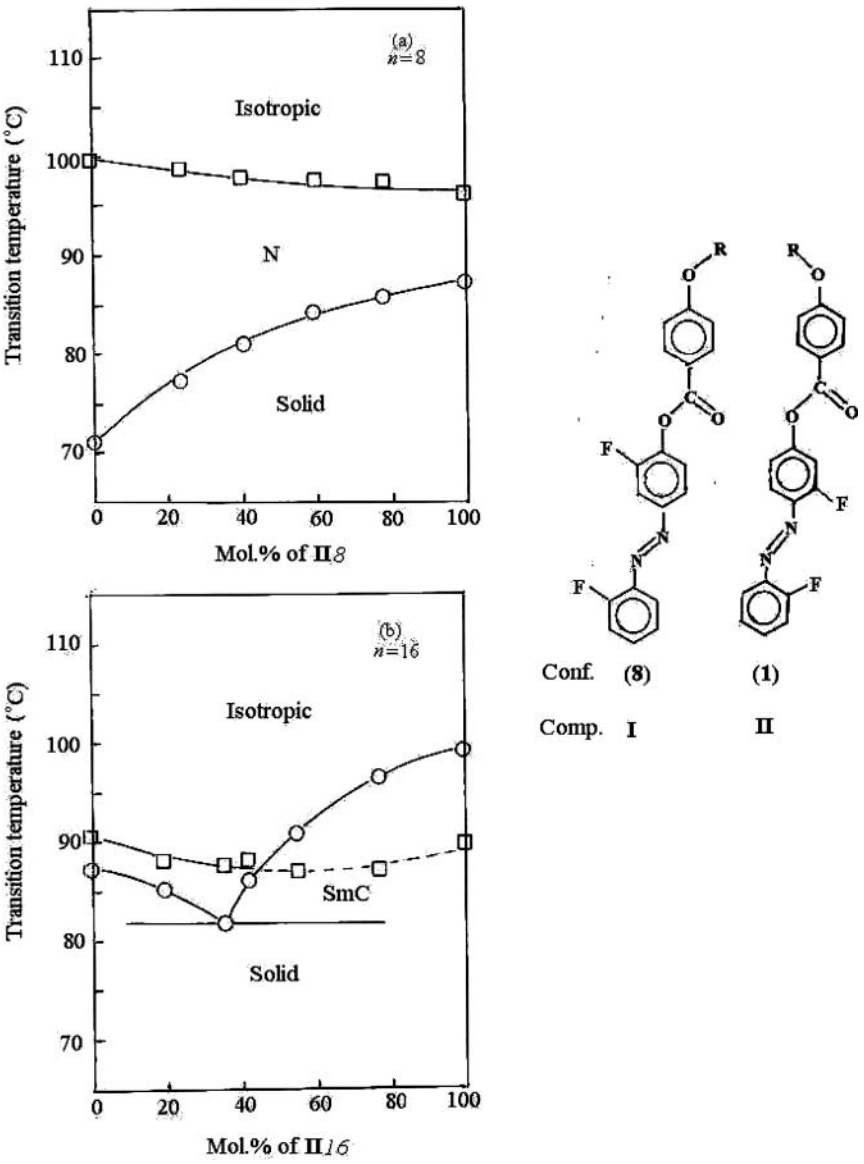

Figure 8. Binary phase diagrams of the systems (**I***n*/**II***n*): (a) $n = 8$, (b) $n = 16$.

their solid mixtures, the first system (**I***8*/**II***8*) forms a continuous solid composition, while the second (**I***16*/**II***16*) showed eutectic composition. This behavior indicates that the crystal lattices of the two components are not dependent on molecular structure.

3.5.2. Binary Mixtures of Isomers, ***I***n ***/III***n. The binary phase diagrams of the two binary systems, ***I****8* ***/III****8* and ***I****16* ***/III****16*, are illustrated in Fig. 9. In the lower homologous system ***I****8* ***/III****8*, the two components form a continuous solid composition with an ideal nematic behavior since both components are nematogenic. This behavior may have led to a back-to-face alignment of the conformation ***8*** for both components (**I***8* and **II***8*). The reverse holds true for the higher homologous system, **I***16* ***/III****16*, where their mixtures exhibit eutectic composition while in the melt, mesophase separation takes place. This may be attributed to the difference in the mesomorphic nature of the two components of the mixture where the first component **I***16* is nematogenic while the other **III***16* is smectogenic.

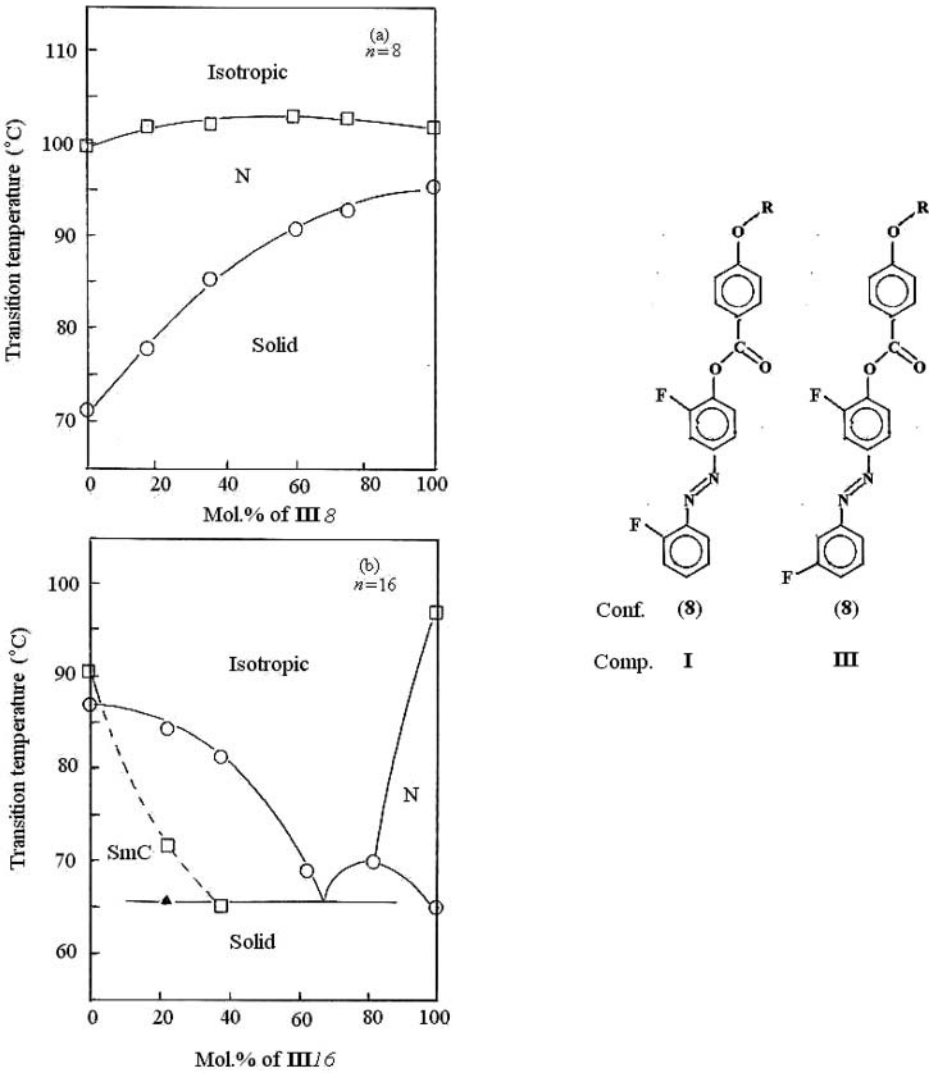

Figure 9. Binary phase diagrams of the systems (**I***n*/**III***n*): (a) $n = 8$, (b) $n = 16$.

*3.5.3. Binary Mixtures of Isomers, **I**n /**IV**n.* The corresponding binary phase diagrams of the two binary systems, **I***8*/**IV***8* and **I***16*/**IV***16*, are illustrated in Fig. 10. In their binary mixtures, the components of the lower homologous system are of different mesomorphic nature in which **I***8* is nematogenic while **I***16* is dimorphic (N and SmC). Accordingly, their mixtures exhibit ideal nematic dependence, evidenced by the linear T_{N-I} composition dependence, while the SmC phase of **IV***8* completely disappeared upon the addition of ≈40 mol% of **I***8*. Their solid mixtures possess a eutectic composition at about ≈40 mol% of **I***8*. On the other hand, since the two components of the higher system **I***16*/**IV***16* exhibit only

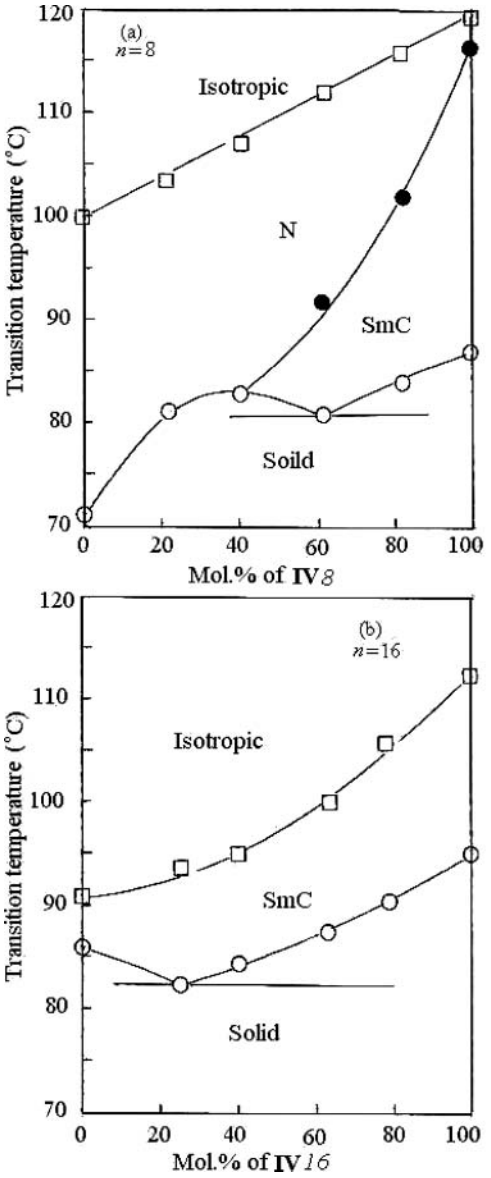

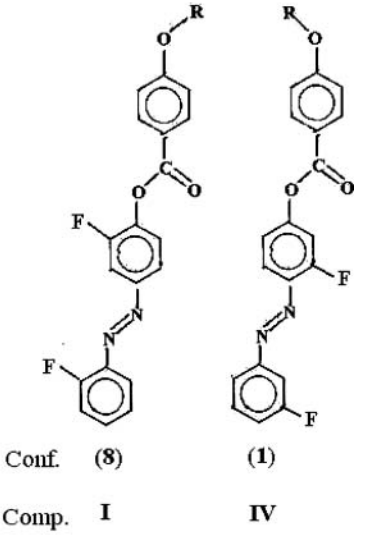

Figure 10. Binary phase diagrams of the systems (**I***n*/**IV***n*): (a) $n = 8$, (b) $n = 16$.

the SmC phase, their mixture showed an ideal mesophase behavior. Eutectic composition is also shown by this system. The ideal mesophase composition behavior may be rationalized through a back-to-face alignment of the conformer ***8*** (for **I***n*) and ***1*** (for **IV***n*). As mentioned above, the fluoro-substituent is not very different in size to the hydrogen it replaces, so it will not cause a significant steric effect in the alignment of the two isomeric components.

3.5.4. Binary Mixtures of Isomers, ***II****n* ***/III****n.* The binary phase diagrams of the two binary systems, **II***8***/III***8* and **II***16***/III***16*, are illustrated in Fig. 11. For the lower system **II***8* **/III***8* both components are nematogenic, hence their mixture exhibits ideal mesophase behavior

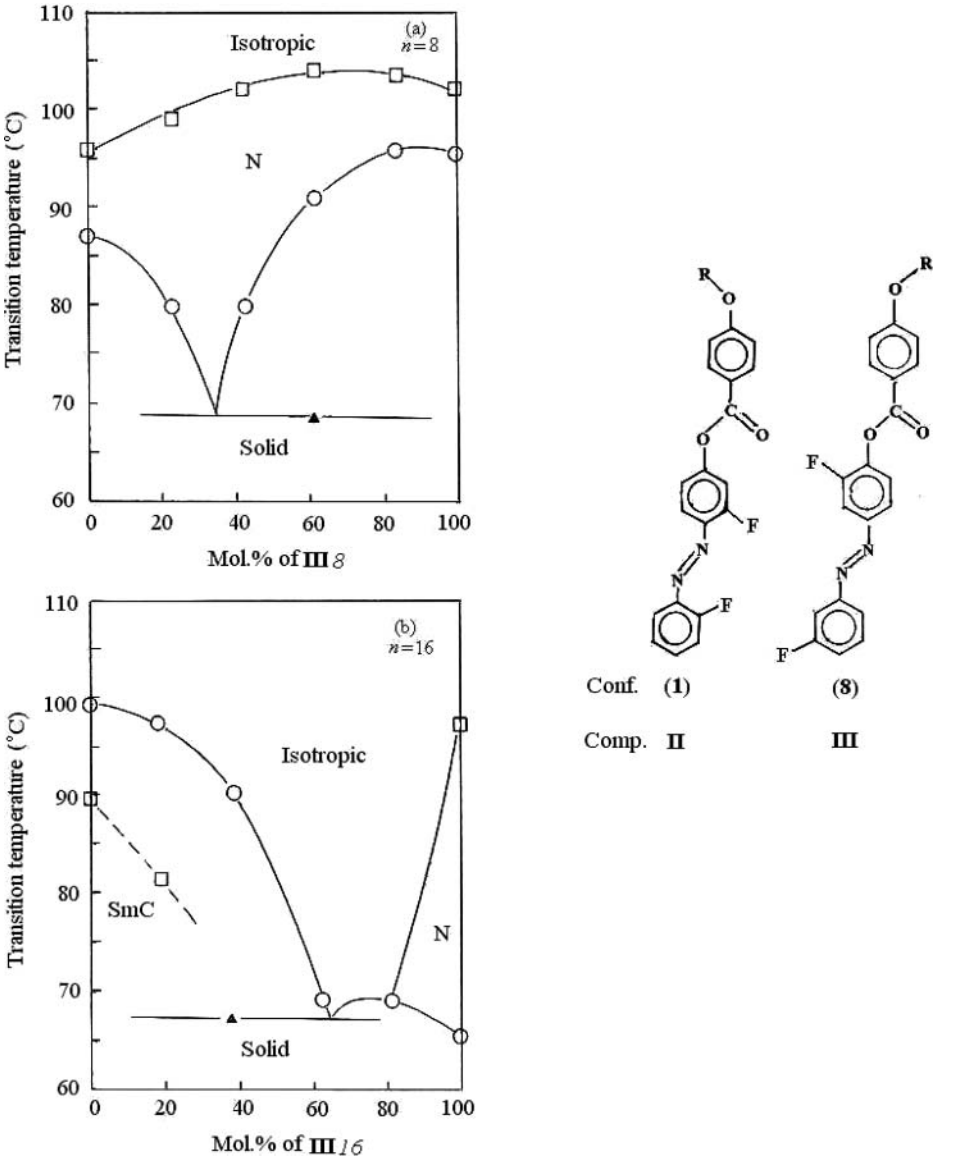

Figure 11. Binary phase diagrams of the systems (**II***n*/**III***n*): (a) $n = 8$, (b) $n = 16$.

with eutectic solid composition. A back-to-face arrangement is probable. Conversely, the mesophase of the higher homologous mixture suffers mesophase separation since the component **II***16* is smectogenic while **III***16* is nematogenic.

3.5.5. Binary Mixtures of Isomers, ***II****n* ***/IV****n.* The binary phase diagrams of the two binary systems, **II***8***/IV***8* and **II***16***/IV***16*, are illustrated in Fig. 12. In the lower homologous

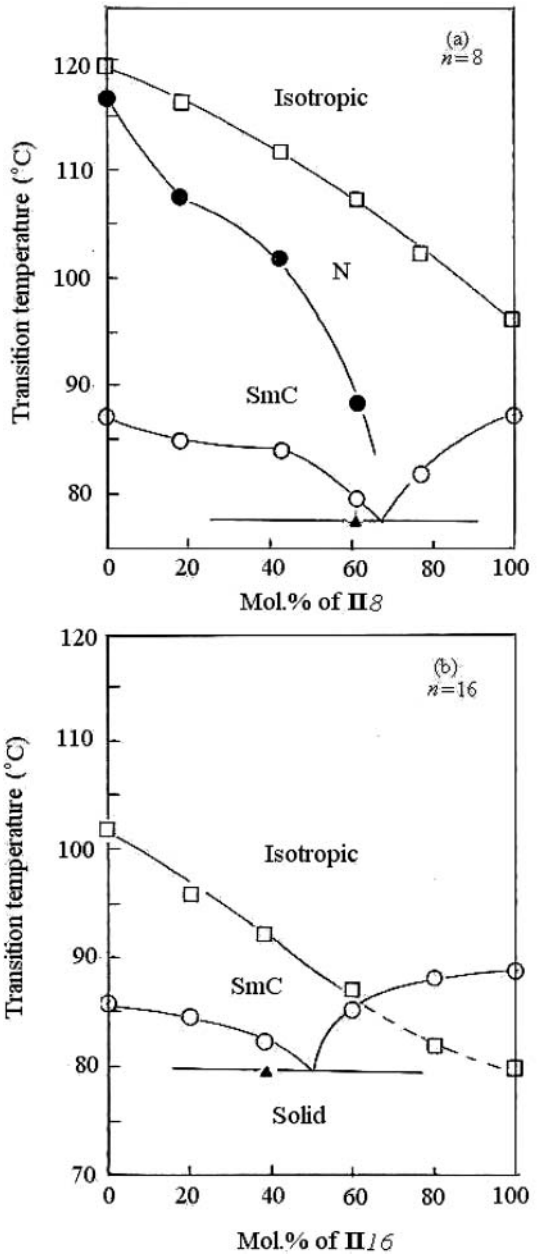

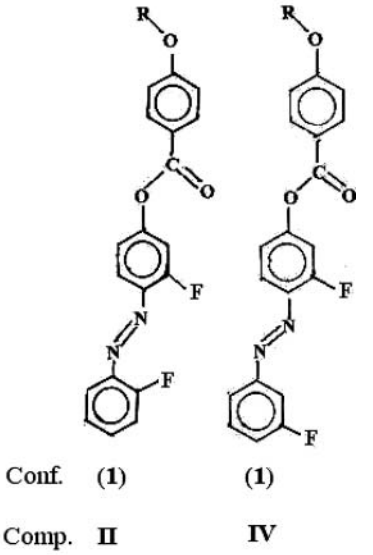

Figure 12. Binary phase diagrams of the systems (**II***n*/**IV***n*): (a) $n = 8$, (b) $n = 16$.

mixture **II***8*/**IV***8*, the component **II***8* is nematogenic while the other component **IV***8* is dimorphic (N and SmC). Accordingly, their mixture shows an ideal nematic behavior with the disappearance of the SmC phase of **IV***8* upon addition of about 40 mol% of **II***8*. In the other system, **II***16*/**IV***16*, both components exhibit the SmC phase, and as a result their mixture exhibits an ideal SmC composition dependence. A back-to-face arrangement is quite suitable to explain such ideal behavior. In both systems, eutectic composition was detected.

*3.5.6. Binary Mixtures of Isomers, **III**n /**IV**n.* The binary phase diagrams of the two binary systems, **III***8*/**IV***8* and **III***16*/**IV***16*, are illustrated in Fig. 13. As with the previous system,

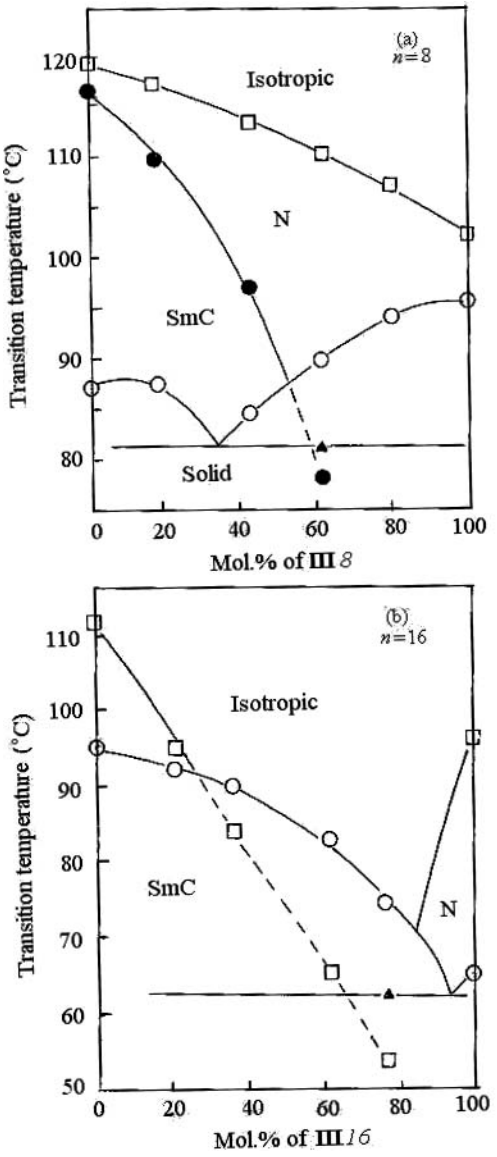

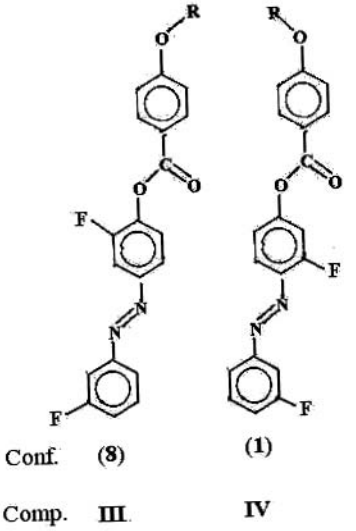

Figure 13. Binary phase diagrams of the systems (**III***n*/**IV***n*): (a) $n = 8$, (b) $n = 16$.

the lower homologous mixture showed ideal nematic-composition dependence, while the SmC phase of **IV***8* disappears upon addition of about 60 mol% of **III***8*. Also, the difference in the mesophase characteristics of the two components of the higher homologous system has caused mesophase separation. Both systems showed eutectic composition.

4. Summary and Conclusions

Four homologous series of the laterally di-fluoro substituted derivatives, 4-(2′-(or 3′-) fluoro phenylazo)-2-(or 3-) fluoro phenyl-4″-alkoxybenzoates, were prepared. These compounds were investigated for their mesophase behavior in pure and mixed states.

The second lateral fluorine atom introduced into the central benzene ring increases further the lateral dipole moment as well as disrupting the symmetry of the molecules thus generating molecular tilting to various extents. Combining the added properties of the two lateral fluoro-substituents, significant changes were observed in the mesomorphic behavior of the compounds and their binary mixtures. Varying extents of mesomeric interactions between the central fluoro-substituent and the ester C=O group, depending on its position, are reflected on the resultant dipole moments, and consequently on their mesomorphic properties.

Various conformations were deduced for the four homologous series via measurement of the dipole moment and comparing it with those theoretically calculated for the various linear planar conformations. The conformations deduced were found to vary according to the relative position of the two fluorine atoms attached to the central and terminal rings.

Binary phase diagrams were constructed for binary mixtures of two isomers (with $n = 8$ and 16 carbons) of the same skeletal structure except for the position of two lateral fluoro-substituents.

Except for the two systems **I***8*/**II***8* and **I***8*/**III***8*, all binary mixtures investigated were found to exhibit eutectic compositions with relatively low melting points that vary between 60°C and 80°C dependent on the relative position of the two fluoro-substituents on each of the two components of the mixture. Investigation of the binary mesophase behavior revealed that the two molecules of most of the binary mixtures investigated are arranged in a back-to-face pattern.

References

[1] Weissflog, W., & Demus, D. (1983). *Cryst. Res. Technol.*, *18*, 21.
[2] Weissflog, W., & Demus, D. (1984). *Cryst Res. Technol.*, *19*, 55.
[3] Weissflog, W., & Demus, D. (1985). *Mol. Cryst Liq. Cryst.*, *129*, 235.
[4] Gray, G. W. (1962). *Molecular Structure and Properties of Liquid Crystals*, Academic Press: New York.
[5] Goodby, J. W., Saez, I. M., Cowling, S. J., Gasowska, J. S., MacDonald, R. A., Sia, S., Watson, P., Toyne, K., Hird, M., Lewis, R. A., Lee, S. E., & Vaschenko, V. (2009). *Liq. Cryst.*, *36*, 567.
[6] Gray, G. W., Hird, M., Lacey, D., & Toyne, K. J. (1989). *J. Chem. Soc. Perkin Trans.*, *2*, 2041.
[7] Chan, L. K. M., Gray, G. W., & Lacey, D. (1985). *Mol. Cryst. Liq. Cryst.*, *123*, 185.
[8] Chan, L. K. M., Gray, G. W., Lacey, D., & Toyne, K. J. (1988). *Mol. Cryst. Liq. Cryst.*, *158*, 209.
[9] Glendenning, M. E., Goodby, J. W., Hird, M., & Toyne, K. J. (1999). *J. Chem. Soc. Perkin Trans.*, *2*, 481.
[10] Cammenga, H. K., Eysel, W., Gmelin, E., Hemmiger, W., Hoehne, G. W. H., & Sarge, S. M. (1993). *Thermochim. Acta*, *219*, 333.

[11] Weissberger, A., & Proskauer, E. (1955). *Organic Solvents, Physical Constants and Methods of Purification*, Clarendon Press: Oxford.
[12] Naoum, M. M., Shinouda, H. G., Shawali, A. S., & Rizk, H. A. (1981). *J. Chim. Phys.*, *78*, 155.
[13] Naoum, M. M., Saad, G. R., Nessim, R. I., Abdel-Aziz, T. A., & Seliger, H. (1997). *Liq. Cryst.*, *23*, 789.
[14] Saad, G. R., & Nessim, R. I. (1999). *Liq. Cryst.*, *26*, 629.
[15] Minkin, W. I., Osipove, O. A., & Zhdanove, U. A. (1970). *Dipole Moments in Organic Chemistry*, Plenum Press: New York.
[16] Zahn, C. T., & Miles, J. B. (1928). *Phys. Rev.*, *32*, 497.
[17] Hedestrand, G. (1929). *Z. Phys. Chem.*, *2B*, 424.
[18] Palit, S. R., Banerjee, B. C. (1951). *Trans. Faraday Soc.*, *47*, 1299.
[19] Castiglione, F., Emsley, J. W., Hird, M., & Street, I. M. (2002). *Phys. Chem. Chem. Phys.*, *4*, 4921.
[20] Dewar, M. J. S., & Griffin, A. C. (1975). *J. Am. Chem. Soc.*, *97*, 6665.
[21] Del Re, G. (1958). *J. Chem. Soc.*, 4031. Poland, D., & Scheraga, H. A. (1967). *Biochemistry*, *6*, 3791. Gasteiger, J., & Marsili, M. (1980). *Tetrahedron*, *36*, 3219. No, K. T., Grant, J. A., & Scheraga, H. A. (1990). *J. Phys. Chem.*, *94*, 4732. No, K. T., Grant, J. A., Jhou, M. S., & Scheraga, H. A. (1990). *J. Phys. Chem.*, *94*, 4740. Park, J. M., No, K. T., Jhou, M. S., & Scheraga, H. A. (1993). *J. Comp. Chem.*, *14*, 1482.